QUALITATIVE ASSESSMENT OF STRUCTURAL DAMAGE DUE TO UNDERGROUND EXPLOSION

Rajesh Prasad Dhakal, Protective Technology Research Centre, School of Civ. & Struct. Engg., Nanyang Technological University, Singapore
Tso-Chien Pan, Protective Technology Research Centre, School of Civ. & Struct. Engg., Nanyang Technological University, Singapore
Shengrui Lan, Defence Science and Technology Agency, Singapore

Abstract

This paper investigates numerically the response of a reinforced concrete frame to explosion-induced ground motions simulated at different distances from the explosion source. The results indicate that nearby structures might experience sudden shear failure and distant structures might undergo less severe damage due to high frequency response that causes larger strain in spite of smaller displacement.

keywords: explosion induced ground motion, high frequency response, inhabited building distance, shear failure, structural damage

1. Introduction

Storing ordnances in the form of weapons, ammunitions, and explosives is an integral part of the defence strategy of each country. Accidental explosion of such ammunitions may cause significant damage to the nearby structures. Hence, it is necessary to regulate the construction of residential structures in the vicinity of ammunition arsenals or underground explosive storage facilities. In other words, the closest permissible distance of residential buildings from such magazines, termed as the inhabited building distance (IBD), should be manifested in the specifications.

In general, the current practice is based on NATO regulations [1]. Equations proposed in these regulations to recommend IBD were based on analyses and tests conducted between the mid-1950s and the mid-1970s. Obviously, there are uncertainties in the present state-of-the-art, and further research in this field is necessary to identify the areas of technical uncertainties and to determine which of these could lead to significant economic paybacks if the degree of uncertainties is reduced. Due to space, costs and safety issues, experimental investigation of structural response and damage due to underground explosions is usually not feasible. That is why very few tests [2] have been conducted in the past few decades, and experimental data in this field are scarce. This leaves numerical simulation a more appropriate alternative. This comprehensive numerical study aims to investigate the effects of underground explosions on the nearby buildings, and comprises of: (i) simulation of explosion-induced ground motion (EIGM) and (ii) investigation of building hazards due to an EIGM.

2. Explosion Induced Ground Motions

As most of the explosion tests conducted in the past [3, 4] are of small-scale and the recorded ground excitations are unable to cause remarkable damage even to very close structures, more rational way is to generate large-scale EIGMs through numerical simulations. It is believed that an EIGM depends on many factors such as quality and quantity of explosives, depth of charge, surrounding soil properties, distance from the source, etc. As an extensive investigation with due consideration to all these parameters is out of scope, EIGM data simulated at different distances for one representative explosion condition [5] are used in this study. Altogether, six ground excitations corresponding to the horizontal and vertical motions simulated at 50, 100 and 150 m from a large-scale explosion source are considered. As a representative case, the acceleration time history of horizontal ground motion simulated at 50 m distance and its Fourier transform are shown in Figure 1. Other five ground motions are not shown but the important parameters (such as the peak particle

velocity PPV, peak ground acceleration PGA and frequency content) of these ground excitations are listed in Table 1.

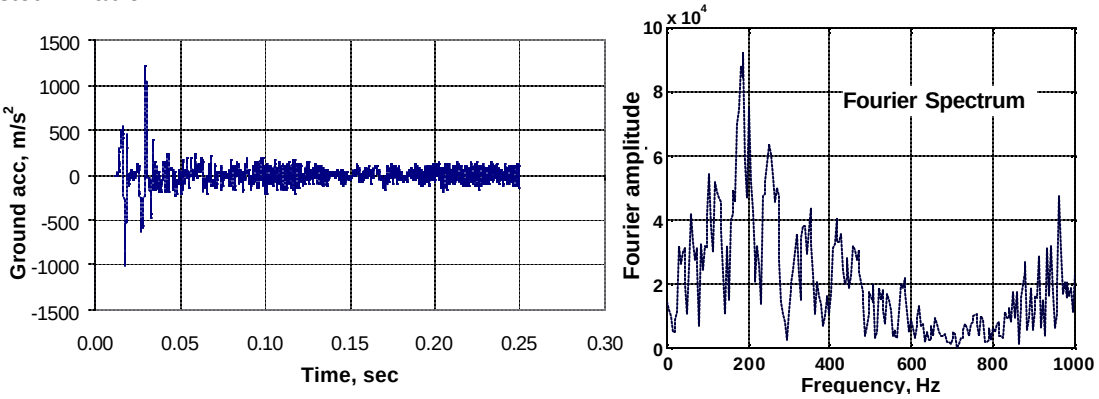

Figure 1. Typical EIGM obtained through simulation (horizontal excitation at 50 m distance)

Table 1. Characteristics of simulated EIGMs

Distance, m (Direction)	PPV, m/s	PGA, m/s^2	Frequency range, Hz	Frequency at peak, Hz
50 (Horizontal)	0.978	1220.19	<1200	188.65
100 (Horizontal)	0.580	428.89	<800	105.72
150 (Horizontal)	0.426	343.16	<500	103.65
50 (Vertical)	0.874	1234.61	<700	209.61
100 (Vertical)	0.288	340.87	<600	148.00
150 (Vertical)	0.238	241.87	<500	128.53

These numerically generated EIGMs consist of relatively short excitations with a large amplitude and high frequency. Moreover, the vertical excitation is found to be significant and non-negligible in comparison with the horizontal one. From Table 1, it is evident that PPV and PGA of the simulated ground motions decrease with the increase in distance but the rate of decrease becomes less prominent as the distance increases. It was also found that the very high frequency contents gradually disappear as the distance increases but the dominant frequency band is almost unaffected by the distance in spite of the change in the frequency at the peak. This information will be helpful in qualitatively generating EIGMs to represent different distance through interpolation/extrapolation.

3. Numerical Investigation

Apart from the nature of EIGM, the type of structure also influences the extent of damage due to an underground explosion. For example, an explosion may be hazardous for a weak building and, at the same time, harmless for a stronger building. In this study, a typical two-storey reinforced concrete building frame is considered and nonlinear finite element analysis is conducted on the representative frame to qualitatively investigate the influence of underground explosion on building structures. Though this study is not sufficient to explicitly formulate general IBD recommendation, it undoubtedly provides a fair idea regarding the response mechanisms and probable failure types of RC buildings at a different distance from the explosion source.

3.1 Representative structure

The layout of the representative two-storey reinforced concrete building frame and its geometrical details are shown in Figure 2. This frame supports one side of a 150 mm thick slab (5 m×5 m) rested on the beam in each floor. The dead load of the floor is equal to 25 KN/m^3, and live load of 7.5 KN/m^2 is assumed to act on the floors. The mechanical properties of concrete are assumed as follows: compressive strength f_c' = 30 MPa; tensile strength f_t = 2 MPa; Poisson ratio ν = 0.2; compressive strain at peak strength ε_p = 2400 $\mu\varepsilon$; and elastic modulus E_c = 24.8 GPa. Similarly, the properties of steel reinforcement are adopted as follows: yield strength f_y = 410 MPa; ultimate strength f_u = 615 MPa; breaking strain ε_u = 5%; and Young modulus E_s = 200 GPa. Assuming the beams to be rigid in axial direction and modelling the frame as two degree of freedom system, fundamental frequencies for the first two global transverse vibration modes are computed as 1.8 Hz and 4.88 Hz, respectively. Similarly, the vertical structural frequency is found to be 27Hz. Moreover, a preliminary computation

shows that the transverse vibrations of the beams and columns have fundamental frequencies around 4.3 Hz and 43.3 Hz, respectively.

The shear capacity of the section is the sum of the shear contributions of concrete and web reinforcement. The shear carried by the web reinforcement can be computed by the well-known truss analogy and that by concrete can be computed by an empirical equation [6]. Finally, the shear capacity of the section turns out to be equal to 171.9 KN. Similarly, the moment capacity computed according to section analysis is equal to 107.75 KN-m. These capacities should be compared with the induced shear force and bending moment to decide on the mode of failure or the safety margin that qualitatively reflects the extent of damage.

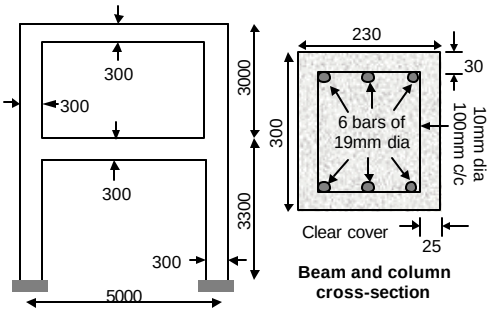

Figure 2. Representative 2-storey RC frame

3.2 Analytical tool and constitutive models

A three-dimensional nonlinear finite-element analysis program called COM3 (*C*oncrete *M*odel in *3*D) [7] is used for numerical investigation. In COM3, the nonlinear dynamic computation is based on direct integration method. The columns and beams are discretized using three-dimensional frame elements, which are analysed by fibre technique [8]. The two-storey RC frame is discretized into 60 elements (i.e. 10 elements for beams and columns in each storey) and each element consists of 220 parallel fibres. Depending on the position of each fibre in the cross-section, a fibre may contain either concrete only or both concrete and reinforcing bars. The response of each fibre is computed using average stress-strain relationships of concrete and reinforcement including loading, unloading and reloading components that are fully path-dependent [9]. It is to be mentioned here that these nonlinear material models give due consideration to bond between concrete and reinforcing bars and also the cover concrete spalling as well as reinforcement buckling mechanisms. These constitutive models are experimentally verified at the material and structure level with sufficient accuracy for static and dynamic analysis of reinforced concrete [9].

The beam-column joint is modelled as a part of the column in the analysis. As the live load and dead load of the floors are transferred to the columns through the beams, they are uniformly distributed through the length of the beams. Total axial load on each column due to the live load on the slab and weight of slab and beams turns out to be 160 KN, which is around 7.7% of its axial capacity. Fixed supports are provided at the bases of both columns and EIGMs simulated for horizontal and vertical directions are applied simultaneously at these supports. The out-of-plane direction effect and short duration blasting wave propagation effect are not considered in this analysis.

4. Results and Discussions

4.1 Structural response to EIGM simulated at 50 m

First, the RC frame is simultaneously subjected to the vertical and horizontal EIGMs simulated at 50 m from the explosion. The horizontal and vertical responses (displacement and acceleration) throughout the loading duration at different points in the frame are extracted from the output. Similarly, the induced shear force and bending moment histories at the base of the left column are also extracted.

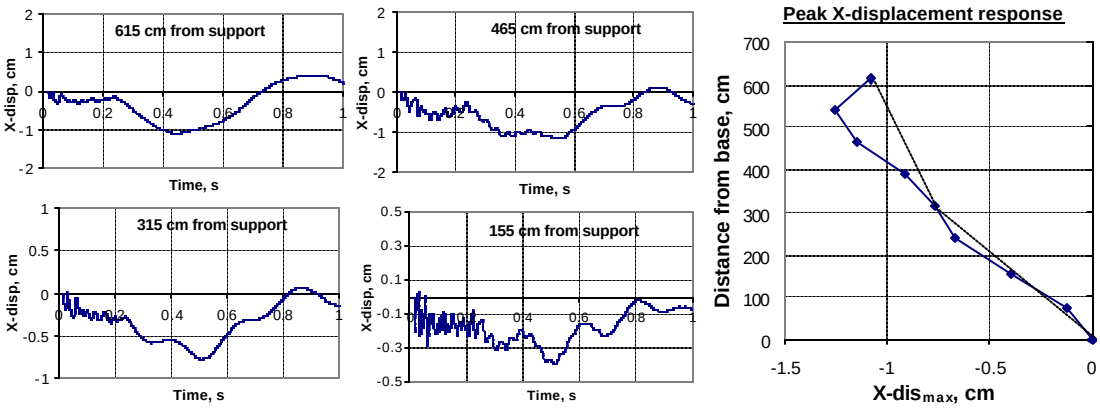

Figure 3. Lateral displacement of different points along the left column

Lateral displacement histories at different points in the left column are shown in Figure 3. The absolute maximum lateral displacement profile of the left column is also included in Figure 3. As lateral displacements at different points in the column reach the maximum value almost simultaneously (i.e. around 0.5 s), the maximum displacement profile closely represents the displaced shape at the most critical condition. Due to a short loading duration, the maximum lateral displacements occur in the free vibration phase, and that at the top of the frame is around 11 mm, which corresponds to less than 0.2% average storey-drift. As the displacement histories suggest, the roof vibrates in fundamental global mode but oscillation of the second floor seems to include high frequency modes. As suspected, the displacement histories of column-centres in each storey indicate the presence of local vibration modes that have a shorter natural period (i.e. higher fundamental frequency). Existence of local vibration mode can also be justified from the maximum lateral displacement profile. The dashed line in Figure 3 represents the global mode, and column displacement from this line is the contribution of local modes, which is more prominent in the second storey. It can be observed that most of the global lateral displacement is concentrated in the first storey and relative drift of the second storey is much smaller. Similarly, Figure 4 shows the maximum lateral acceleration of different points in both columns normalized with respect to horizontal PGA. It shows that acceleration response is higher in the second floor than in the roof, and the peak accelerations at intermediate points in the columns are much larger than those at floor levels. This also corroborates that the columns respond with higher frequency modes than the floors.

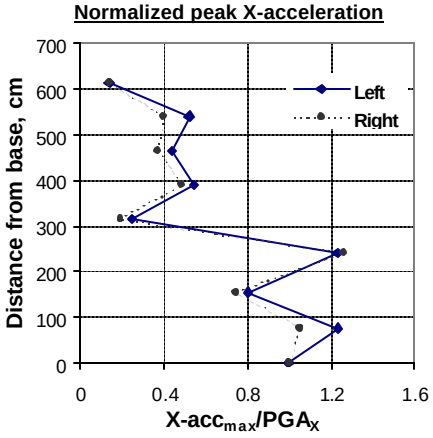

Figure 4. Normalized maximum lateral acceleration profile along the columns

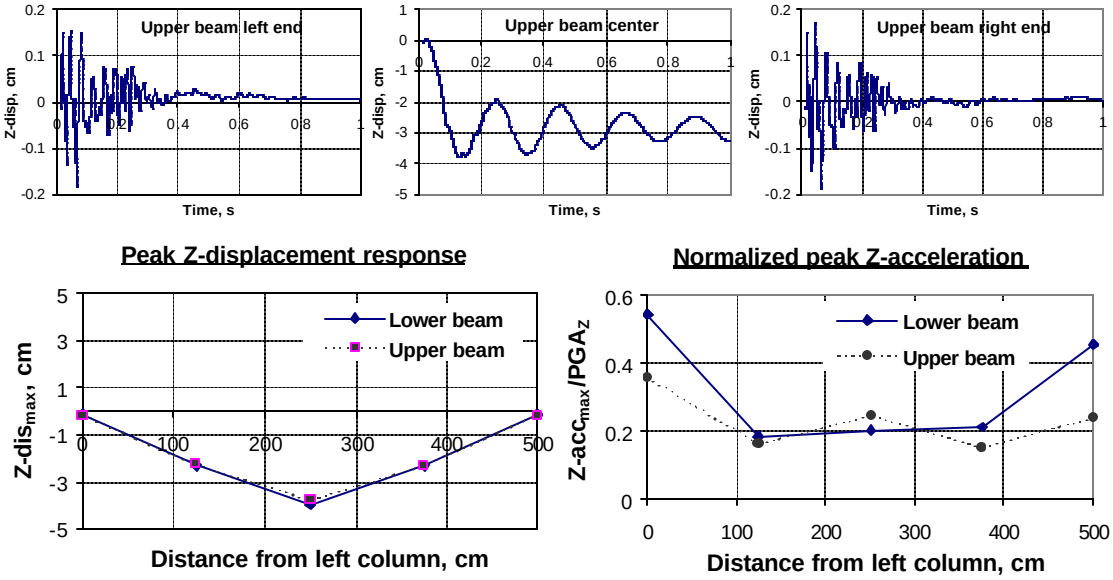

Figure 5. Vertical displacements of different points along the beams

Figure 5 illustrates the vertical displacement histories at different points of the beam in the roof. Moreover, the maximum vertical displacement profiles and the normalized acceleration profiles are also included in Figure 5. The displacement patterns of beams in the two floors resemble with each other. A maximum downward displacement of around 40mm occurs at the centre of the beam but the vertical responses at the beam-ends show a significantly small displacement. Moreover, the maximum vertical acceleration profile also shows that the peak accelerations at the beam-ends are more than those at intermediate points. Both of these observations indicate that the beam-ends follow the global vertical mode that has a higher fundamental frequency due to the large axial stiffness of columns, but

the beam vibrates in its local mode, which has a comparatively longer natural period (i.e. lower fundamental frequency).

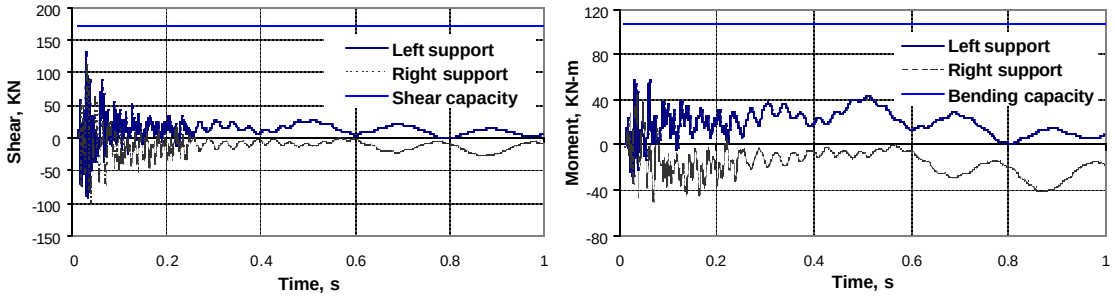

Figure 6. Shear force and bending moment induced at the base of columns (50 m EIGM)

Figure 6 illustrates the comparison of induced shear force and bending moment at the base of both columns with the corresponding capacities computed by section analysis. The comparisons show that neither shear nor moment has reached the predicted threshold values. Note that the induced shear force becomes maximum during the forced vibration phase, and the shear capacity corresponding to a higher loading rate is not necessarily equal to the one predicted earlier. During a high frequency excitation, the contribution of concrete will increase due to increase in the material strength but the stirrups may not contribute as the shear cracks are expected to be straight rather than inclined at 45^{o}, as assumed in the truss analogy. Consequently, overall shear capacity is expected to decrease slightly.

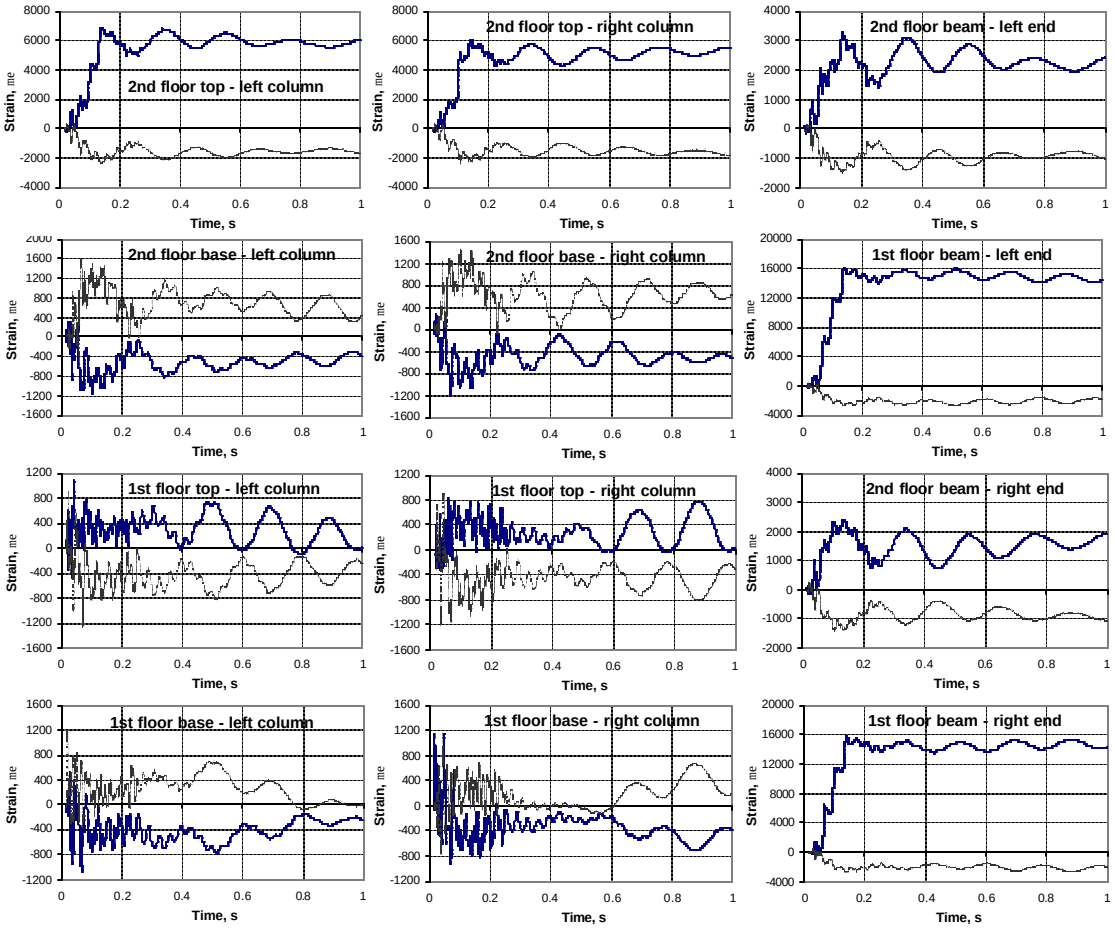

Figure 7. Extreme fibre strains at critical locations in the frame

As mentioned earlier, structural response not only consists of the fundamental global mode but also includes significant contributions from global and local vibration modes with higher frequency. Due to high frequency modes, structures might experience damage in spite of a small overall displacement. Consequently, conventional seismic damage assessment methods based primarily on displacement response are not suitable for explosion-induced damage assessment. To get qualitative idea regarding the extent of damage, strain histories of extreme fibres at some critical locations (i.e. near joints) are extracted and shown in Figure 7. As can be seen, fibre strains at some locations are larger than yielding strain (≅2000 με), especially at the beam-ends and at the top of both columns in the second storey. Hence, possibility of wider cracks and section deterioration at these locations cannot be ruled out. As fibre strains in all of the selected locations exceed cracking strain (≅150 με), small cracks are expected to occur throughout the frame.

4.2 Structural response to EIGMs simulated at 100 m and 150 m

Next, the same RC frame is subjected to the vertical and horizontal EIGMs simulated at 100 m and 150 m, respectively. Though not shown in detail, responses in both cases are found to be qualitatively similar to those due to 50 m EIGM. Needless to mention, induced shear force and bending moment are much less than the corresponding capacities, and the possibility of shear failure does not exist at all. Lateral displacements are smaller, e.g. storey-drift due to 100 m EIGM is around 0.1%. As in previous case, high frequency vibration modes could be noticed in the response histories. Consequently, in spite of very small storey-drift, strains are found to be non-negligible, especially in the beams and at the top of the columns. The maximum and minimum values of extreme fibre strains at some critical locations are shown in Figure 8. Localized damages are expected at the beam-ends in the first storey and some sporadic cracks are expected in other parts as well. For 150 m EIGM, numerical results show that strains at all locations are less than yielding strain. Hence, the frame does not experience any damage although few fine cracks may appear at some locations. Based on these numerical results, it can be said that the typical two-storey RC building frame adopted in the analysis can bear without failure the simulated explosion at a distance of 100 m or more though few smeared cracks might appear.

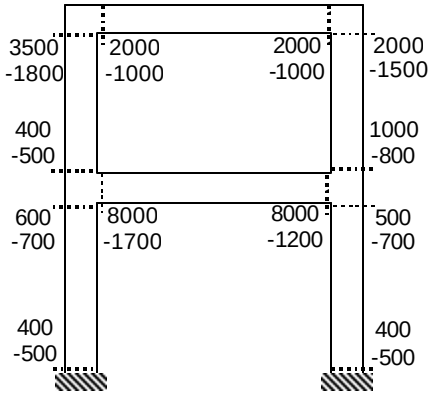

Figure 8. Extreme fibre strains in με corresponding to 100 m EIGM

4.3 Structural response to extrapolated EIGM

Next, the same RC frame is subjected to two times the EIGM data simulated at 50 m from the explosion source. This extrapolated data may represent either one or both of the following conditions: (i) ground motion simulated at a closer distance from the explosion source, and (ii) ground motion induced by a larger amount of explosive.

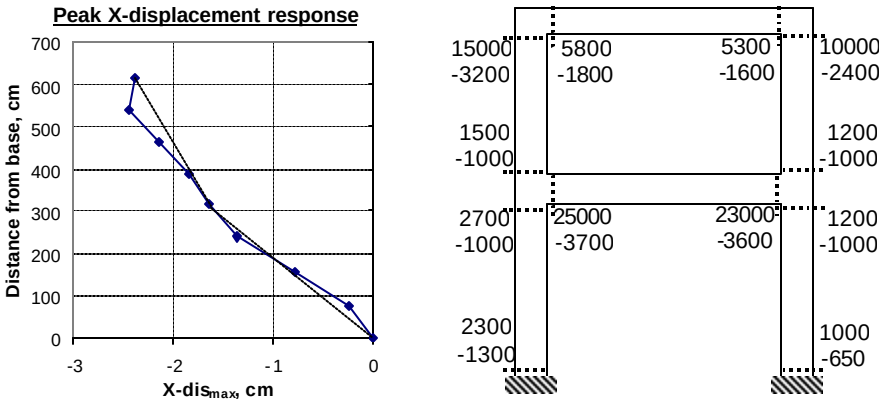

Figure 9. Maximum displacement and extreme fibre strains in με (2×50 m EIGM)

As shown in Figure 9, the lateral displacement at the first floor level is around 1.7 cm (i.e. 0.5% storey-drift). Recalling the extent of damage corresponding to much smaller displacements in previous

cases, it can be fairly predicted that extensive damage may occur in the beams and columns. The maximum and minimum fibre strains in some locations of the frame are also illustrated in Figure 9. As expected, it can be noticed that strains are much larger than in previous cases and the frame might experience severe damage. It is to be reminded that the maximum displacement response occurs in free vibration phase whereas the induced shear becomes maximum during the forced vibration phase. Shear force and bending moment induced at the base of the columns throughout the analysis domain are compared with the corresponding capacities in Figure 10. It can be observed that bending moment is less than the flexural capacity but shear force is higher than the shear capacity. Considering that actual shear capacity during a high frequency loading might be slightly less than the predicted static shear capacity, it can be said that shear failure is highly likely to take place in the forced vibration phase. The frame may collapse due to sudden shear failure during the explosion before being damaged due to high frequency structural response in the post-explosion free vibration phase.

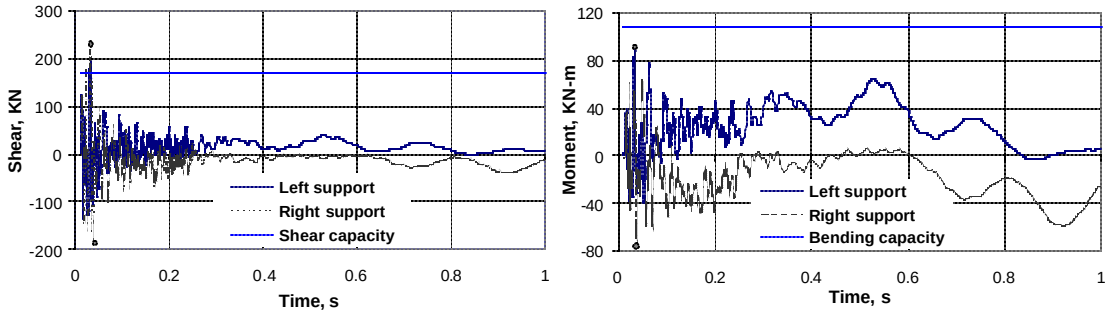

Figure 10. Shear force and bending moment induced at the base of column (2×50 m EIGM)

4.4 Qualitative assessment of structural safety

Based on the aforementioned numerical results, overall safety of typical RC buildings located at different distances from the source of explosion of different amount of explosives can be qualitatively assessed. Usually, the characteristic distance (i.e. distance normalized with respect to the third root of explosive mass in kg) is used as the abscissa to draw the attenuation curves so that a single curve can be used for any combination of distance and explosive amount. However, the authors believe that it is inappropriate to generalize the explosion-induced structural damage using the conventional normalization technique. For example, a structure subjected to the explosion of a significantly large explosion experiences substantial damage if it is not very far from the explosion source. In contrast, the same structure subjected to very small amount of explosive cannot be damaged, regardless of its distance from the explosion source. Hence, it becomes imperative to discuss the attenuation of structural damage separately for different explosion scales.

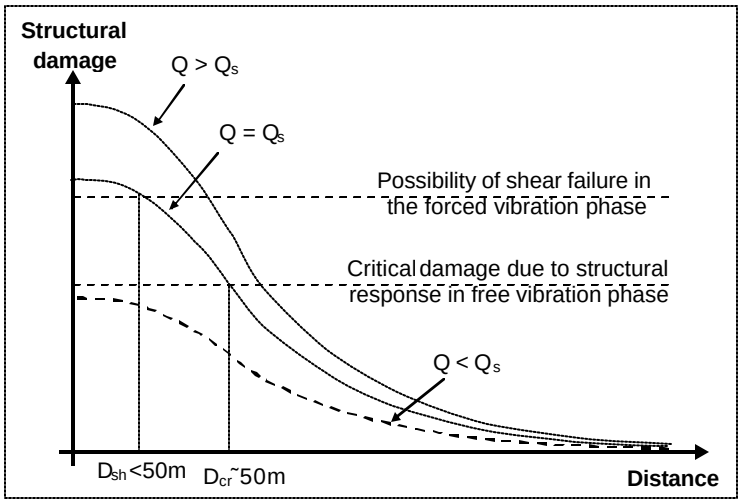

Figure 11. Schematic representation of structural safety against underground explosion

Figure 11 illustrates schematically the relationship between structural damage and the distance between the structure and the explosion source. The solid line in Figure 11 corresponds to the damage corresponding to simulated explosive quantity Q_s. The other two dashed lines in the figure represent cases with more and less amount of explosives. The figure indicates that the safety of structures far from explosion source is always guaranteed regardless of the amount of explosive. For closer structures, two damage mechanisms are identified. Structures very close to the explosion source may undergo a sudden shear failure of some of its components during the forced vibration phase. As this type of failure is governed by induced shear force that in turn depends on input energy or impulse, the frontier of shear failure zone depends primarily on the amount of explosive. For considerably small quantity of explosive, the shear failure zone may not exist at all. Structures outside the shear failure zone can reach the free vibration phase, where they may experience damage due to the high frequency response (i.e. local vibration modes of individual member and higher order global vibration modes) that causes larger strains in spite of small displacements. The degree of overall damage can be quantified by adopting appropriate damage index and comparing the computed damage index with index-ranges corresponding to low, moderate and severe damages.

5. Conclusions

In this study, the qualitative relationship between the safety of reinforced concrete building and its distance from an explosion source is established through numerical approach. First, horizontal and vertical explosion induced ground motions (EIGM) simulated for 50 m, 100 m and 150 m from the explosion site of 250 tonnes of TNT, were used as input ground excitations. Next, a two-storey reinforced concrete building frame was selected to represent common RC buildings. Finally, the non-linear finite element analyses were performed with the simulated and extrapolated vertical and horizontal EIGMs applied simultaneously at the base of the representative RC frame.

Based on the simulated EIGMs, it can be concluded that EIGM has some special characteristics such as significantly higher frequency, larger amplitude and shorter duration. Due to the impulsive nature of EIGM, the maximum displacement response of a structure usually occurs in the free vibration phase. Hence, analyses aimed to predict structural response to underground explosion are recommended to cover a time domain much longer than the loading (i.e. EIGM) duration. Due to the high frequency loading components, vibration pattern of the RC frame includes higher frequency global and local modes causing the overall displacement response to be small. However, the fibre strains are large enough to cause damage in some parts of the frame in spite of a small storey-drift. For frames subjected to magnified EIGMs, the shear force induced during the ground excitation exceeded the shear capacity of the columns. Hence it can be concluded that for structures closer to a larger-scale explosion source, sudden shear failure of some members may take place during the forced vibration phase due to the excessive input energy/impulse. Note that the probability and active range of shear failure zone as well as the structural damage zone depend on the amount of explosive.

References:

[1] North Atlantic Treaty Organization, *Manual on NATO Safety Principles for the Storage of Ammunition and Explosives*, Document AC/258-D/258, Brussels, 1999.

[2] Skjeltorp, A., *Underground Ammunition Storages: Model Tests to Investigate External Safety Distances*, Fortifikatorisk Notat 36/67, Norwegian Defence Construction Service, Oslo, 1967.

[3] Zhao, J., Wu, Y.K., Cai, J.G., Chen, S.G. and Zhao, Y.H., *Small–scale Ground Shock Tests at the Mandai Quarry*, Technical Report to the Lands and Estates Organization, Ministry of Defence, Singapore, 1997.

[4] Murrell, D.W. and Joachim, C.E., *The 1996 Singapore Ground Shock Test*, Waterways Experiment Station, Department of Army, Vicksburg, 1996.

[5] Ma, G.W., Hao, H. and Zhou, Y.X., Modelling of Wave Propagation Induced by Underground Explosion, *Computers and Structures*, 1998, 22 (3-4), 283-303.

[6] Japanese Society of Civil Engineers, *Standard Specification for Design and Construction of Concrete Structures*, JSCE, Tokyo, 1996.

[7] Maekawa, K., Irawan, P. and Okamura, H., Three-Dimensional Constitutive Laws of Reinforced Concrete, *International Conference on Applied Concrete Mechanics APCOM*, Seoul, 1996.

[8] Menegotto, M. and Pinto, P.E., *Method of analysis of cyclically loaded RC plane frames including changes in geometry and non-elastic behaviour of elements under normal force and bending*, Preliminary Report No. 13, IABSE, 1973, 15-22.

[9] Okamura, H. and Maekawa, K., *Nonlinear Analysis and Constitutive Models of Reinforced Concrete* , Gihodo, Tokyo, 1991.